ANNUAL ANALYSIS WITH UAV AUTOMATIC NAVIGATION FOR ONIGI RICE TERRACES IN HASAMI TOWN

Yukiya TANIGUCHI, Haruhiro HIDAKA, Takashi NAGAFUCHI, Susumu OGAWA
Civil Engineering and Environmental department, Nagasaki University
E-mail. bb35515021@ms.nagasaki-u.ac.jp, ogawa_susumu_phd@yahoo.co.jp

KEY WORDS：GIS, Land cover, NDVI, NDWI, Photogrammetry

ABSTRACT: Life and livelihood of Onigi rice terraces declined by cultivation abandonment and crop conversion in Hasami town. As the rice terraces were developed on the slopes, the area in rice terraces is small and productivity is lower than flatland paddy fields. Therefore, understanding the conditions of the vegetation, water balance and land uses is important for Onigi rice terraces. Land cover maps are required in many places including rice terraces since 66% of Japan is covered with forests. On the other hand, in recent years, spread of a UAV progressed rapidly. A UAV was used in many fields. Images of a UAV are higher resolution than aerial photographs of satellites, and the photographs could be repeated easily. Land cover classification of vegetation and water areas can be done from RGB and infrared images. UAV has automatic navigation functions, and the air dose rate was measured even in places where human intrusion was difficult. In this study, annual analysis of land covers was carried out with UAV automatic navigation for Onigi rice terraces in Hasami Town. First, a UAV route map of Onigi rice terraces was made with automatic navigation software. Next, since April of 2017, a UAV flew over the rice terraces. 5-band images of visible range, near infrared, and short wavelength infrared were acquired with IR filters. 3D models and orthographic images were created from these 5-band aerial images. Spatial distributions of NDVI, NDWI and land covers were calculated with GIS software from the orthographic images. Their seasonal changes were examined from calculated NDVI, NDWI spatial distribution.

1. INTRODUCTION

On Onigi rice terraces existing in Hasami-town, agriculture is declining. Farm work by machines and people entering are difficult because the rice terraces exist in in a sloping ground. The rice terraces growth control is inferior to that of flat paddies [1]. Therefore, grasping the time series changes of the vegetation, the moisture contents and land cover classification in the rice terraces are inquired. On the other hand, in recent years, the spread of a UAV progressed rapidly. A UAV became popular in the fields of earth science and archeology [2]. Compact digital cameras mounted on UAV are much higher resolution than aerial photographs of traditional aircrafts. The shooting was repeated spatially [2]. UAV was used for a long flight by general users in high performance of batteries, the weight reduction of aircrafts, and higher precision of GPS and IMU [3]. Small size GPS automatic recording systems with high portability, and general versatility were installed at low cost, and the air dose rate was measured. Spatial dose distribution was measured over places where the access was difficult by a small UAV [4]. Photogrammetry with automatic navigation can be done in complicated terrains. The aerial images become three-dimensional using SfM-MVS software. High-resolution terrain images were obtained and analyzed [2]. Ortho mosaic images and DSM of

several-cm-level spatial resolution were obtained from 3D models [4]. By computing these data with GIS software, landslide collapses, vegetation, and hydrological balance were analyzed. In this study, creating the land cover classification maps and the time series changes of the vegetation, the moisture contents were examined using UAV automatic navigation in Onigi rice terraces from April 2, 2017 to September 18, 2017.

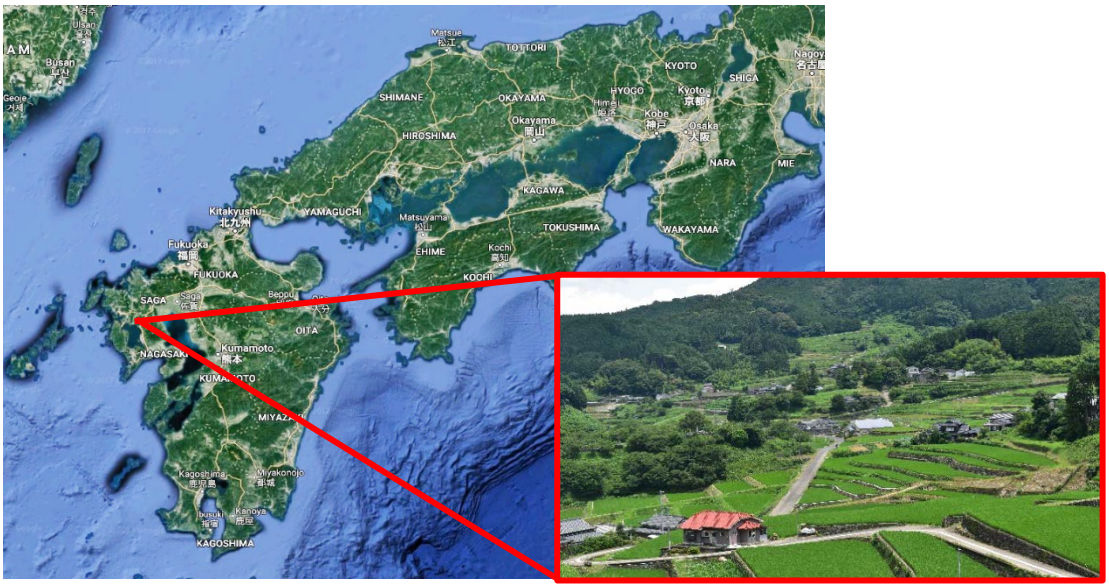

Figure 1. Horizontal image in Onigi rice terrace.

2. METHODS

2. 1. Automatic navigation map

In this study, *Litchi for DJI Mavic / Phantom / Inspire / Spark* was used to create automatic navigation route map of Onigi rice terrces. The UAV route map is shown in Figure 2. For all routes, the altitude was fixed at 150-m. The speed was set to 28 km / h. On July and September survey, the camera was set to automatically shoot every 2 seconds. The flight time was 21 minutes and the flight distance was 7.6 km to make the consumption of the battery within 70%.

Figure 2. UAV route map using *Litchi* for Onigi rice terraces.

2. 2. *Phantom 4* and *Phantom 4 Professional*

Phantom 4 and *Phantom 4 Professional* were used in this study (Figure 3). On April 2 and 23, June 10, July 22, and September 18, 2017, the authors visited Onigi rice terraces in Hasami-town. Aerial images of RGB, near infrared and short wavelength infrared were taken by the UAV. The infrared images was taken by attaching infrared films with the UAV lens cover.

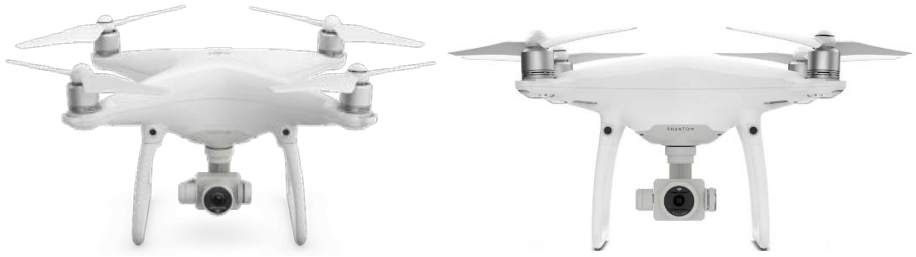

Figure 3. *Phantom 4* and *Phantom 4 Professional*.

2. 3. 3D analysis

Based on 6-dimensional information of the images color and GPS from the obtained aerial images, 3D models were created using PhotoScan. If alignment and high-density cloud construction are "high" or more, the analysis takes a huge amount of time because the number of images was large and the shooting range was wide. In addition, 3D construction might have concentrated on places where photographing was frequent. Therefore, in this study, all alignment and high-density cloud construction were set to "low" or "medium". This analysis was done each RGB, near infrared and short wavelength infrared. Synthetic orthophotos with were created from these three dimensional models.

2. 4. GIS analysis

2. 4. 1. NDVI and NDWI

Spatial distribution maps of NDVI and NDWI were created from orthophotos of RGB, near infrared and short wavelength infrared using ArcGIS subtraction. NDVI means *Normalized Difference Vegetation Index*. This is vegetation index calculated using the difference between red in visible light and near infrared. Plants absorbed much red light and reflected much near infrared light. The vegetation distribution maps were created by subtracting the red images from the near infrared images by subtracting the red of RGB image from the near-infrared image. NDWI means *Normalized Difference Water Index*. This is moisture content index calculated using the difference between red in visible light and short wavelength infrared. Water did not reflect short wavelength infrared light. The moisture content distribution maps were created by subtracting the short wavelength infrared images from the red of RGB image. The calculation formula for both of NDVI and NDWI were shown in (1)-(2). Band 3 was red color of visible light. Band 4 was near infrared. Band 5 was short wavelength infrared.

$$NDVI = \frac{Band4 - Band3}{Band4 + Band3} \quad (1) \qquad NDWI = \frac{Band3 - Band5}{Band3 + Band5} \quad (2)$$

2. 4. 2. Land cover classification maps

From April data, Land cover classification diagram were created with two ways of supervised learning and unsupervised learning. In supervised learning, a land cover classification map were created by extracting some samples with manual using RGB orthophoto. In unsupervised learning, another land cover classification map were created with auto combining RGB, near infrared, and short wavelength infrared orthophotos.

3. RESULTS

Figures 4-7, and 9 shows the distribution maps of RGB images, NDVI, NDWI for Onigi rice terraces from April 2 to September 18, 2017. Figures 8-10 shows horizontal images of RGB, NDVI, and NDWI obtained with a digital camera on July 15 and September 18, 2017. Figure 11 shows land cover classification maps with "supervised learning" and "unsupervised learning" by April data.

3.1. NDVI

From Figures 4-10, NDVI changes from April to September, NDVI was low in the rice terraces until June. In July data, NDVI was high after rice planting was completed. Differences between places with and without rice were identified in NDVI distribution maps. In NDVI horizontal images of Figures 8 and 10, the vegetation index of July data was higher than that of September data.

3.2. NDWI

In Figures 4-5, from NDWI distribution maps, the moisture contents for the rice terraces were calculated higher than the surrounding mountainous area. From June to September, NDWI distributions did not been created. In the horizontal images of NDWI in Figures 8 and 10, the soil and the road part reacted more strongly than the rice terraces.

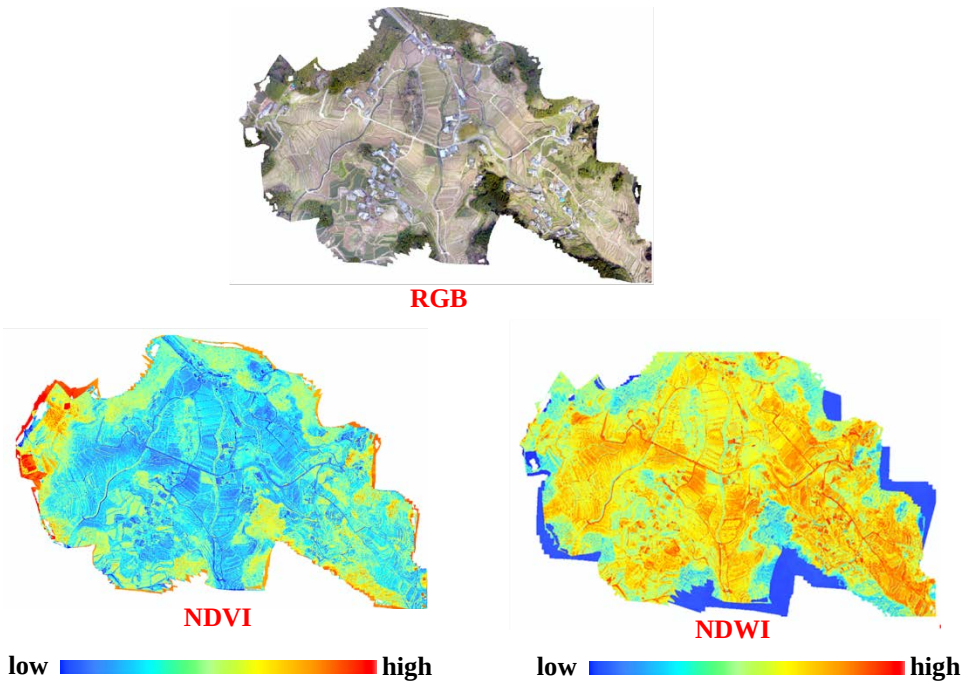

Figure 4. RGB, NDVI and NDWI distributions on April 2, 2017.

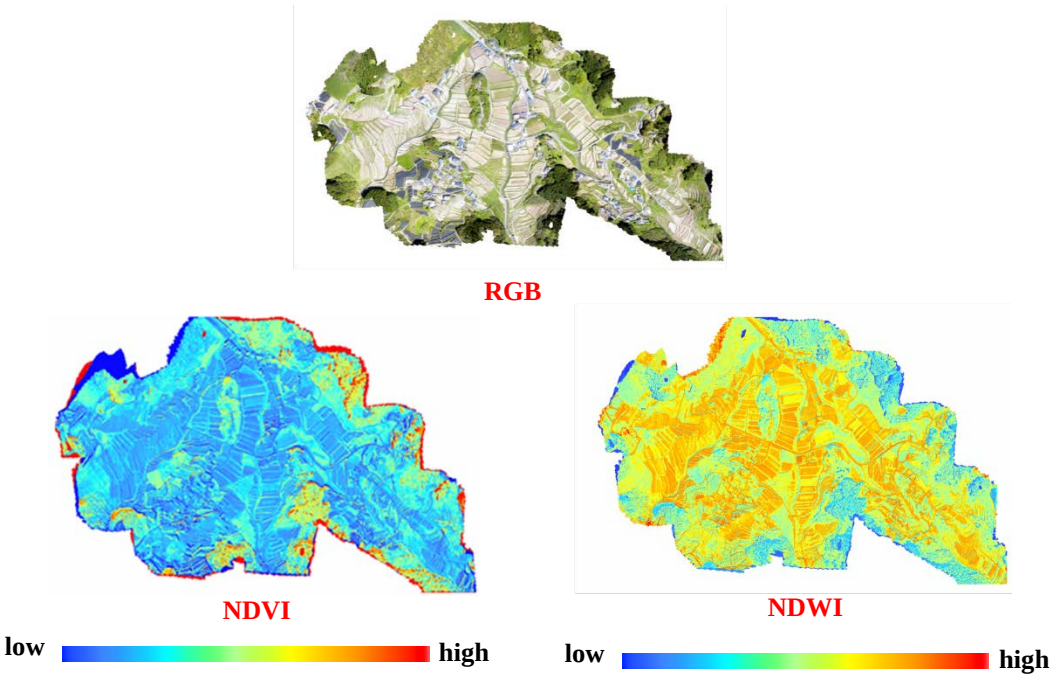

Figure 5. RGB, NDVI and NDWI distributions on April 23, 2017.

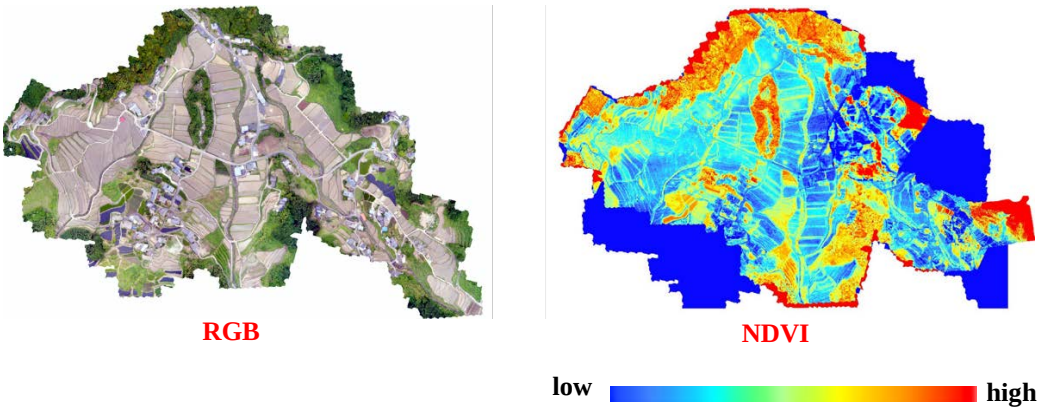

Figure 6. RGB and NDVI distributions on June 10, 2017.

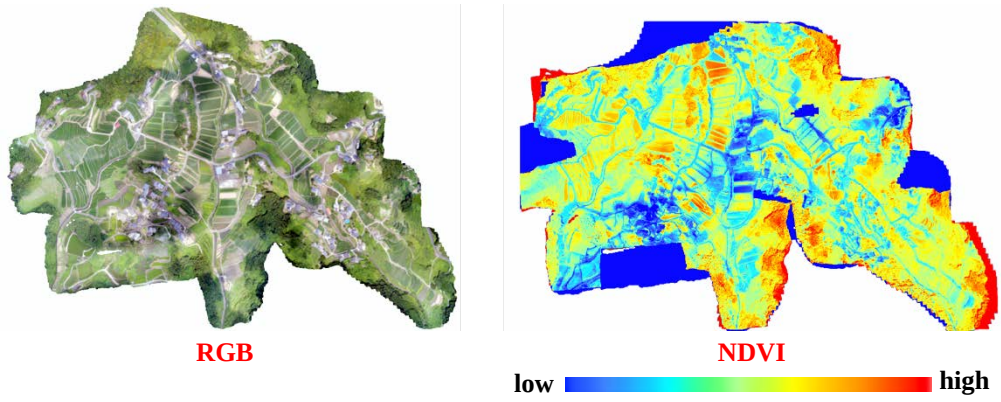

Figure 7. RGB, NDVI and NDWI distributions on July 22, 2017.

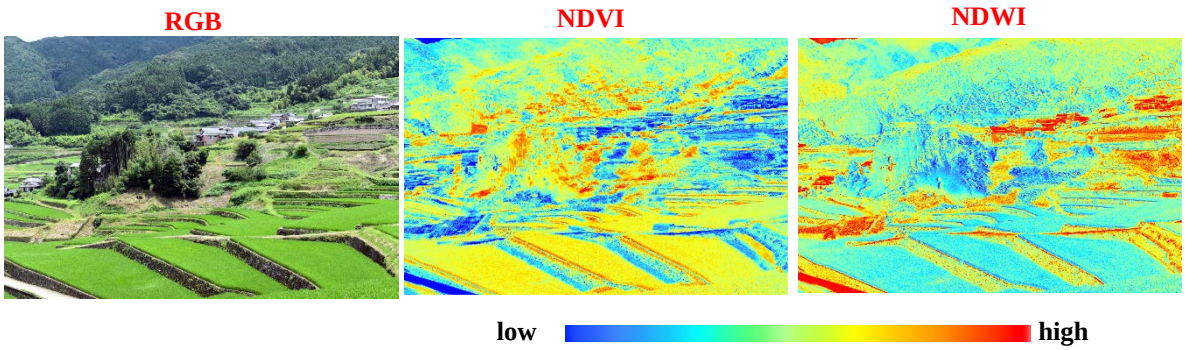

Figure 8. Horizontal images of RGB, NDVI and NDWI distributions on July 15, 2017

Figure 9. RGB distributions on September 18, 2017

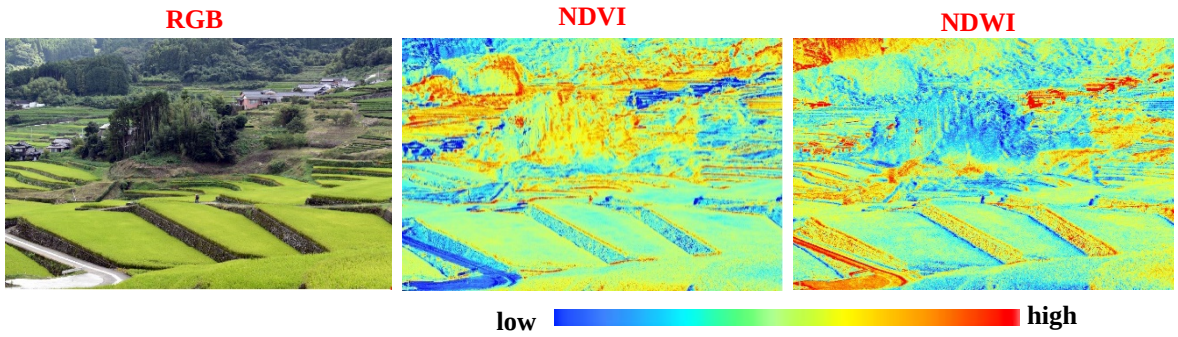

Figure 10. Horizontal images of RGB, NDVI and NDWI on September 18, 2017.

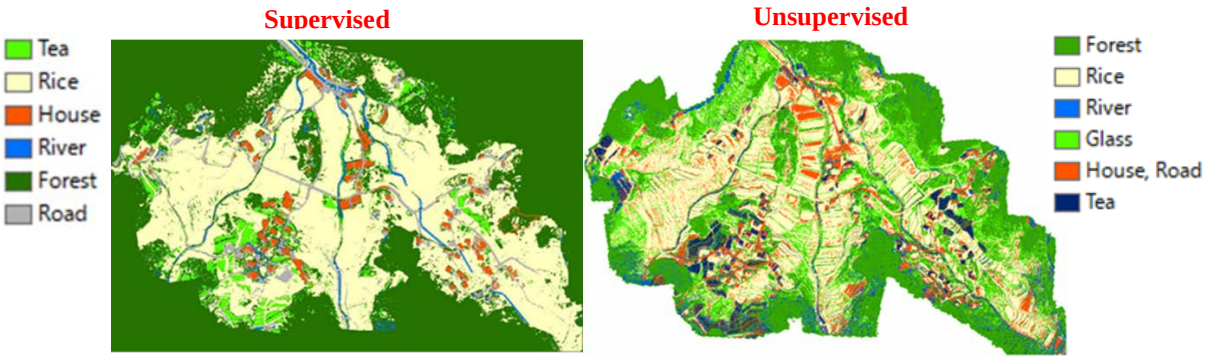

Figure 11. Land cover classification map

4. DISCUSSION

4. 1. NDVI

In April data, NDVI distributions were created in all area. Meanwhile, in June and July, there were blue parts in several places outside. This were parts where 3D models of near-infrared images were not obtained by camera vibration, darkness. Compared with RGB images, infrared images are more likely to vibration and dark. In September data, a 3D model of near -infrared images was created. However, some errors occurred in NDVI distribution because weather was cloudy. If the shooting part is shadowed, infrared light reflectance become weaker.

4. 2. NDWI

In NDWI distribution maps of Figures 4-5, rice terraces were calculated higher than the surrounding mountainous area. Clay was used for soil in paddy fields. The moisture contents of the soil for rice terraces were higher than other places. Therefore, NDWI distributions of rice terraces were higher on April. In NDWI of Figure 10, soil area were higher than vegetation area because soil area had more moisture contents than vegetation area. Acquisition of RGB and Short-wavelength-infrared images using a UAV would be applied to creation of soil quality maps. In NDWI of Figure 9, the road reacted higher. For NDWI formula, when red color reflects more, the NDWI become higher. NDWI of the roads became higher because the red color reflection of the roads was higher than other areas. From June to September, NDWI was not calculated. Infrared images were difficult to take in a cloudy day, and the camera setting of the exposure amount and focus were incompatible with shooting in short-wavelength-infrared. Vegetation and moisture content analysis using a UAV were easier than airplanes. However, adverse effects by clouds are large, and a sunny day was optimal.

4.3. Land cover classification map

For land cover classification maps in both of supervised learning and unsupervised learning, such as rice fields, houses, rivers, forests were classified at high resolution. Classifications of forest coniferous and deciduous trees or each house by the material were not identified in detailed points. By doing machine learning programed independently, more accurate land cover classification diagrams would be created without ArcGIS.

5. CONCLUSIONS

Complex terrain survey was measured by a UAV with three-dimensions. Furthermore, the spatial distributions of NDVI and NDWI were obtained. High resolution land cover classification maps were created. In this study, by attaching infrared film in camera lens, arbitrary different wavelengths were taken with one UAV. As a result, the biomass of plants was measured quantitatively from NDVI, and the soil moisture contents were estimated from NDWI in Onigi rice terraces. UAV was lower price, higher resolution and quasi-all-weather-type than satellite images. Therefore, species and biomass quantity per microscale plant and the water balance of evapotranspiration which were not measured with conventional satellite data, and the water balance such as evapotranspiration could be estimated.

REFFERENCES

[1] T. Nagafuchi, Y. Imamura, S. Ogawa, 2017, A study on the landscape characteristic of Onigi rice terraces in Hasami town, *NAOSITE*, 47(89), pp.87-92.

[2] S. Ishiguro, Y. Kumahara, H, Goto, T. Nakata, N. Matsuta, N. Sugino, D. Hirouchi, M. Watanabe, 2016, Evakuation of high-resolution digital surface models of surface rupture associated with the 2014 Kamishiro fault earthquake, central, Japan, using unmanned aerial vehicle photography and SfM-MVS analysis, *Journal of The Remote Sensing Society of Japan*, 36(2), pp. 107-116.

[3] K. Sakai, R. Yamamoto, K. Hasegawa, T. Izumi, H. Matsuyama, 2016, Generation of a DSM of the forest crown by vertical+oblique stereo pair images taken by a small-sized UAV, *Journal of The Remote Sensing Society of Japan*, 36(4), pp. 388-397.

[4] A. Hama, K. Tanaka, H. Yamaguchi, A. Kondo, 2017, Dose rate mapping by small UAV to radioactive contamination area, *Journal of The Remote Sensing Society of Japan*, 37(1), pp. 13-20.

[5] S. Otsubo, S. Ogawa, H. Hidaka, G. Yamada, 2016, Present state of UAV and applications for civil engineering, *NAOSITE*, 46(86), pp. 43-49.

[6] G. Yamada, S. Ogawa, S. Otsubo, and H. Hidaka, 2016, Simulation of disaster research with UAV on Kumamoto Earthquake, *Asian Conference on Remote Sensing*, 37.

[7] S. Otsubo, S. Ogawa, H. Hidaka, Y. Imamura, 2017, Survey on the vegetation cover and irrigation for rice terrace with UAV, *NAOSITE*, 47(88), pp. 7-12.

[8] H. Mizuochi, T. Hiyama, H. Kanamori, T. Ota, Y. Fujioka, M. Iijima, K. K. Nasahara, 2016, Water storage monitoring of seasonal wetlands in a semi-arid environment by the integrated use of long-term satellite images and UAV topography measurement, *Journal of The Remote Sensing Society of Japan*, 36(2), pp. 81-92.

[9] Research Group for High-resolution Satellite Remote Sensing, 2016, High resolution satellite remote sensing for the disaster of the 2016 Kumamoto earthquake, *Journal of The Remote Sensing Society of Japan*, 36(3), pp. 211-213.